

Measurement of the spatio-temporal distribution of harmonic and transient eddy currents in a liquid metal

J Forbriger, V Galindo, G Gerbeth and F Stefani

Forschungszentrum Dresden-Rossendorf, P.O. Box 510119, D-01314 Dresden, Germany

E-mail: F.Stefani@fzd.de

Abstract. Harmonic and transient eddy currents in a liquid metal positioned above an excitation coil are determined by measuring the voltage drop in a simple potential probe. The resulting spatio-temporal eddy current field is compared with the corresponding analytical expressions for a conducting half-space. Further, a deformation of the eddy current distribution due to a non-conducting torus immersed into the liquid metal is measured and compared with numerical results. The method can be generalized to arbitrary geometries, and might help to validate numerical models for non-destructive testing and magnetic inductance tomography.

Keywords: Eddy currents, Magnetic induction tomography, Non-destructive testing, Liquid metals

Submitted to: *Meas. Sci. Technol.*

1. Introduction

Eddy currents play a crucial role in magnetic induction tomography (MIT) [1], in non-destructive testing [2], and in different versions of contactless flow measurements for liquid metals as, for example, in contactless inductive flow tomography (CIFT) [3, 4], in induction flow-metering based on phase shift measurements [5], and in Lorentz force velocimetry [6]. Usually, the eddy currents in the bulk material are indirectly inferred from non-invasive measurements of external induced magnetic fields. The final inverse problem of inferring the material inhomogeneities or flow velocities from the induced magnetic fields is still a formidable task.

In many cases, it would be desirable to have independent eddy current measurements in order to validate numerical solvers for the forward and the inverse problem. For evident reasons, a detailed eddy current measurement in solid materials is hardly possible. Up to present, only some eddy current measurements at the surface of thin solid aluminum plates were reported [7] and served for the validation of a numerical benchmark problem.

In contrast to solid metals, liquid metals are perfectly suited for a full scan of the eddy current distribution in the bulk of the conducting material. Actually, various liquid metals (mercury [8], Wood's metal [9]) have been used already in eddy current testing since they allow an easy defect modelling. However, to the best of our knowledge, in this paper we present the first spatio-temporal measurements of eddy currents in a liquid metal alloy (GaInSn) both for the case of harmonic excitation and for the case of a pulsed (transient) excitation. Whereas harmonic excitations have been used for long in non-destructive testing, the transient excitation has achieved much attention only during the last ten years. Nowadays it is used for non-destructive testing in many areas, including the detection of corrosion and cracks in aging aircrafts fleets [10].

In order to start with an accurate reference model, we determine harmonic and transient eddy currents in a cylindrical vessel which is large compared to the radius and the distance of the exciting cylindrical coil. This problem can be reasonably approximated by the eddy current problem in a conducting half-space for which analytical solutions are known, both in the harmonic and in the transient case [11].

Another measurement is carried out for the more complicated situation that a non-conducting torus with quadratic cross-section is immersed into the liquid metal. These measurements are then compared with numerical results from the commercial FEM software OPERA.

The paper closes with a summary and some conclusions.

2. Theory

2.1. Analytical models

Consider a conducting half-space with conductivity σ and a coil of radius R located at a distance a to the boundary of the half-space (figure 1). Independent of the time-

dependence of the exciting current, the eddy currents in the half-space will only have an axisymmetric azimuthal component $j_\phi(r, z)$.

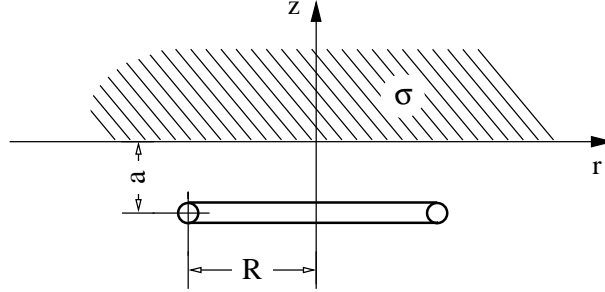


Figure 1. Geometry of the simplified analytical model to determine harmonic and transient eddy currents in the conducting half-space.

First we consider a harmonic current $I(t) = I_0 \sin(\omega t)$ in the coil with amplitude I_0 and angular frequency $\omega = 2\pi f$. In [11], the distribution of the eddy current density $j_\phi(z, r, t)$ in the conducting half-space was shown to have the form

$$j_\phi(z, r, t) = -i\mu_0\sigma\omega RI(t) \int_0^\infty e^{-ka} J_1(kR) J_1(kr) \frac{e^{-qz}}{k+q} k dk, \quad (1)$$

where the abbreviation

$$q = \sqrt{k^2 + i\mu_0\sigma\omega}. \quad (2)$$

is used. J_1 is the Bessel function of order 1 and μ_0 is the magnetic permeability of the free space (throughout the paper we assume the relative magnetic permeability μ_{rel} to be equal to 1).

For each point r, z the integral (1) can be easily evaluated. Typically, we have used discretizations with 50-200 points in the k space, and we have carefully checked the convergence of the integration procedure.

Now let us assume that the current in the excitation coil is suddenly switched on so that it corresponds to a step function $I(t) = I_0\Theta(t)$. Quite similar to the harmonic case, the induced transient eddy current density j_ϕ can be represented as an integral over the wave number k :

$$j_\phi(z, r, t) = -\mu_0\sigma RI_0 \int_0^\infty e^{-ka} J_1(kR) J_1(kr) L(k, z, t) k dk, \quad (3)$$

with J_1 being again the Bessel function of order 1 and $L(k, z, t)$ being defined as

$$L(k, z, t) = \left[\frac{1}{\sqrt{\pi t}} e^{-\frac{\mu_0\sigma z^2}{4t}} - \frac{k}{\sqrt{\mu_0\sigma}} e^{k|z|} + \frac{k^2 t}{\mu_0\sigma} \operatorname{erfc} \left(\frac{k\sqrt{t}}{\sqrt{\mu_0\sigma}} + \frac{\sqrt{\mu_0\sigma} z}{\sqrt{4t}} \right) \right] \times \frac{e^{-\frac{k^2 t}{\mu_0\sigma}}}{\sqrt{\mu_0\sigma}}. \quad (4)$$

The results of equation (1) for the harmonic case and of equations (3,4) for the transient case will be visualized in the following section where we will compare them with the measured current distribution.

2.2. Finite-element models

In addition to the analytical expressions (1) and (3), we also determine the eddy current by the commercial FEM package OPERA. OPERA is a finite element analysis software for time varying electromagnetic fields. It includes a module for solving eddy current problems in which the exciting currents can vary sinusoidally or in another predetermined way in time.

2.3. The measurement

The measurement principle for the eddy currents relies on Ohm's law in non-moving conductors which connects the electric current density \mathbf{j} with the electric field \mathbf{E} via $\mathbf{j} = \sigma \mathbf{E}$. The measured voltage U_{12} between two points P_1 and P_2 can be expressed by the line integral over the electric field $U_{12} = \int_{P_1}^{P_2} \mathbf{E} \cdot d\mathbf{s}$. The only current component that appears in our particular problem is the azimuthal one which can be determined by the voltage between two electrodes whose difference vector points in azimuthal direction. At every instant t and every position r, z , this azimuthal current density $j_\phi(z, r, t)$ can be approximated by

$$j_\phi(z, r, t) = \frac{U_{12}(z, r, t)\sigma}{d} \quad (5)$$

where d stands for the distance between the electrodes. The value of d chosen in the experiment results as a compromise between maximizing the measurable voltage and minimizing the inaccuracies which appear in particular for small radii r .

3. Experimental set-up

The experimental set-up is shown in figure 2. The central part is a cylindrical glass vessel (1) filled with the eutectic alloy $\text{Ga}^{67}\text{In}^{20.5}\text{Sn}^{12.5}$, which has the advantage of being liquid down to temperatures of about 10°C . The physical properties of GaInSn at 25°C are: density $\rho = 6.36 \times 10^3 \text{ kg/m}^3$, kinematic viscosity $\nu = 3.40 \times 10^{-7} \text{ m}^2/\text{s}$, electrical conductivity $\sigma = 3.27 \times 10^6 (\Omega \text{ m})^{-1}$. The non-conducting ring (3) is immersed into the liquid only in the second part of the experiment and is held by one stainless steel rod ($d = 3 \text{ mm}$, $\sigma = 1.3 \times 10^6 \text{ S/m}$) which we assume to be non-essential for the current distribution.

The external magnetic field is generated by a circular coil (2), centered below the vessel (1). This coil consists of 63 turns of a 0.6 mm Cu wire and is wound in such a way that the coil has a nearly circular cross-section. The coil is fed by a precise U-I-converter (HERO PA2024C) controlled by an arbitrary-waveform generator (AD-win-Pro). In the case of harmonic excitation, a current of 1 A amplitude and a frequency of 480 Hz

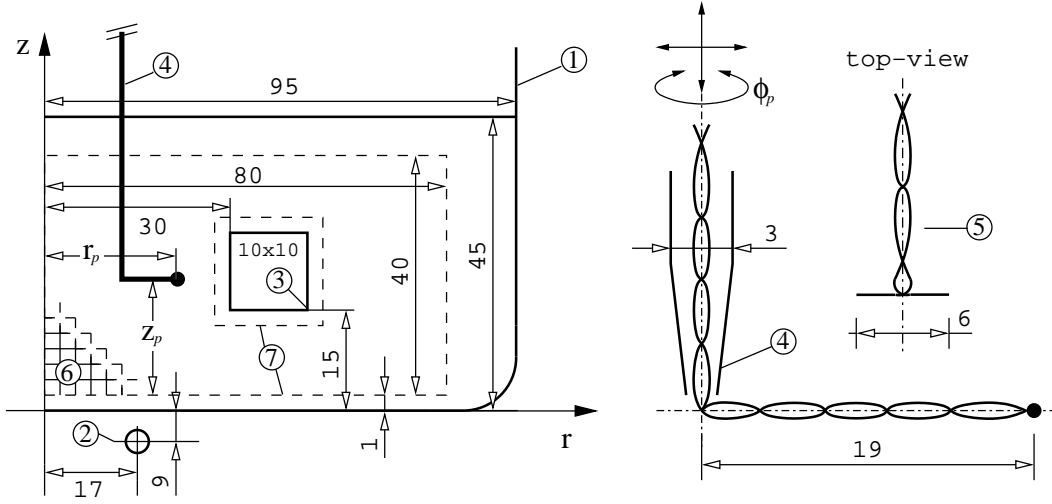


Figure 2. Experimental set-up (not to scale). (1) Glass vessel, (2) excitation coil, (3) PVC ring (only in the second part of the experiment), (4) scanning potential probe, (5) probe in detail, (6) scan-raster, (7) scan-region. All given dimensions are in mm.

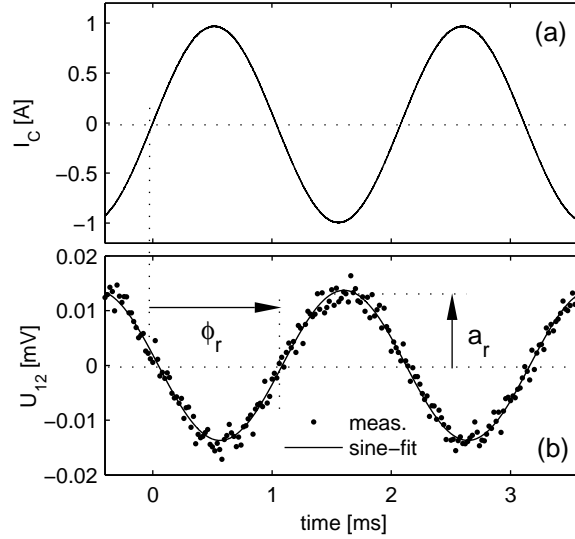


Figure 3. Sample-measurement for harmonic excitation at $r_p = 20$ mm, $z_p = 22.5$ mm. The coil current I_c (a) has an amplitude of 1 A and a frequency of 480 Hz. To determine amplitude and phase-angle of the response-signal $U_{12}(t)$, a sine-function is fitted (least-squares-method) to the data. The resulting parameters $a_r(r_p, z_p), \phi_r(r_p, z_p)$ are the basis for spatial amplitude and phase plots.

was applied to the coil (see figure 3a). In the case of transient excitation, the limited bandwidth of the amplifier requires that the pulse-edges have to be approximated by a continuous function. For this purpose, the 1st quarter-period of $I(t) = I_0(\sin(2\pi ft))^2$ with $I_0 = 5$ A and $f = 2$ kHz was chosen. The resulting rise time (see figure 4) of $t_r = 125 \mu\text{s}$ is small compared to the typical diffusion time of the magnetic field

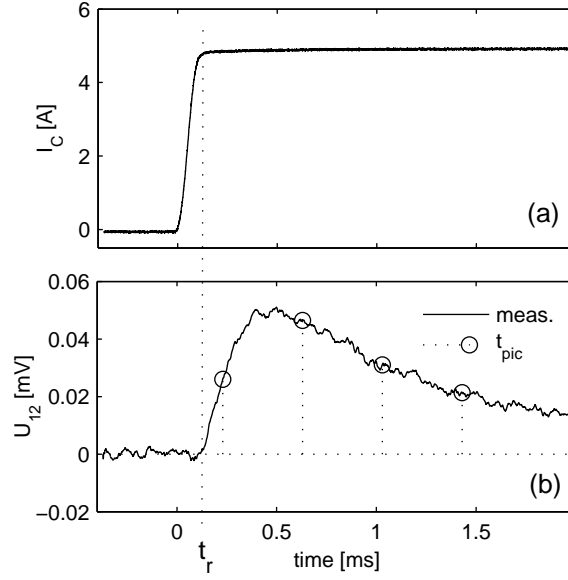


Figure 4. Sample-measurement for pulsed excitation at $r_p = 20$ mm, $z_p = 22.5$ mm. The stem-plots in (b) indicate the instants for which the eddy current distribution will be shown in detail.

$t_{diff} = \mu_0 \sigma R^2 = 1.23$ ms. The pulse duration was set to $t_{on} = 12$ ms, to avoid interactions between the eddy currents resulting from the rising and the falling edge. The pause between the pulses was set to $t_{off} = 100$ ms. This rather long time is necessary to avoid a significant heating of the coil.

The spatio-temporal distribution of the induced eddy current is determined by pointwise measuring the voltage drop $U_{12}(t)$ between the blank ends of two coated wires (0.1 mm Cu-wire) which are twisted to avoid inductive pick-up (r.h.s. of figure 2). The connecting line between the points P_1, P_2 points in azimuthal direction. The wires are guided through a thin glass pipette (4) into the medium. In the top-view of the probe (5) the electrode distance $d = 5.8$ mm is visible. After differential amplification ($g_d = +60$ dB) and low-pass filtering ($f_c = 200$ kHz) the signal is routed directly into a digital storage oscilloscope (Tektronix TDS3034B), which records the response with a sample-rate of 2.5 Megasamples/s over 10 kilosamples. Due to the signal decrease with respect to the coil-probe-distance, the vertical-sensitivity of the oscilloscope is adapted to exploit its dynamic range as good as possible. The entire signal path is realized as a dc-measurement to get correct transients. To specify the exact position (r_p, ϕ_p, z_p) of the potential probe, the pipette is mounted onto a three-axis traversing robot. The ϕ_p -axis is required to make measurements even 'behind' the immersed ring (3) by rotating the probe between 0° and 180° . In order not to deform or crash the probe, a safety distance of 1mm to the vessel and to the ring has been chosen. The extension of the scan-region (7), as well as the spatial resolution (6) are the same for all arrangements to get comparable results. In the present case a step size of $\delta r = \delta z = 1.25$ mm is applied which leads to a raster-size of 65×33 pixels. Thus a measurement time of about 2

hours is necessary to traverse through the whole scan region. The eddy current signal is logged pointwise to a PC which also controls the traversing robot and the waveform generator.

The final eddy current distribution is determined in the post-processing. In the case of harmonic excitation the measured voltages $U_{12}(r_p, z_p, t)$ are fitted by a sine function with the amplitude $a_r(r_p, z_p)$ and the phase $\phi_r(r_p, z_p)$ (see figure 3). For transient excitation, time-slicing through the acquired data results in $u_s(r_p, z_p)$ for each instant (see figure 4). Both fields a_r, u_s are converted from voltage to current by equation (5). To illustrate and compare the measured versus calculated distributions the computation of isolines was performed. The required software was developed under usage of MATLAB (Mathworks Inc.).

4. Results

In this section we compare the measured eddy currents with the analytical results (in the case of homogeneous fluid) and with numerical results (in the case of an immersed torus). It should be noted that the specified lengths in r, z direction refers to r_p, z_p (cp. figure 2). Hence, the shown r -axis is located 1 mm above the boundary of the half space.

4.1. Homogeneous fluid

We start with the case of a homogeneous fluid for which analytical solutions for the harmonic and transient excitation were given in section 2.

4.1.1. Harmonic excitation In the case of harmonic oscillation we show both the amplitude and the phase shift of the induced currents for a frequency of 480 Hz (figure 5).

In addition to the measured values, we show also the results of equation (1). Actually, we have also computed the eddy current by the commercial FEM code OPERA. However, in the adopted spatial resolution the results are indistinguishable from the analytical ones. In general, we see a good correspondence of experimental and theoretical data which expectedly gets worse for smaller radii where the finite distance (6 mm) of the two electrodes of the potential probe makes a precise measurement of the azimuthal currents impossible.

4.1.2. Transient excitation In figure 6 we present the measured and the theoretical eddy current distribution for the case of pulsed excitation for the time instants 200, 600, 1000 and 1400 μ s. These instants were already indicated as circles in the lower panel of figure 4. Again, we observe a good correspondence, despite the used approximations with respect to geometry and to the pulse shape.

It might also be instructive to compare the time evolution of the total currents which is the integral in r and z direction of the eddy current density (figure 7). In a

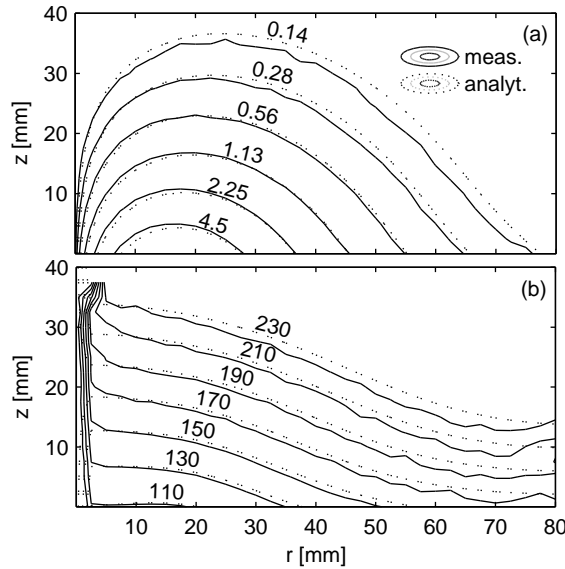


Figure 5. Homogeneous fluid: contour lines of amplitude [A/cm^2] (a) and phase-angle [$^\circ$] (b) of the azimuthal eddy current in the case of harmonic excitation with a frequency of 480 Hz and an excitation current of 1 A.

wide range of the time evolution, the misfit between the two data is of the order of a few percent. Only at the very beginning and at the end (when the measured signal is already very small), we get a discrepancy of around 10 per cent.

4.2. Fluid with an immersed torus

In order to study a slightly more complicated problem which is not solvable anymore by an analytical expression, we have immersed a PVC torus into the liquid metal. This problem has been solved again by means of the commercial FEM solver OPERA which, in the case of a homogeneous fluid, had provided results more or less identical to the analytical one. Note that a similar transient eddy current analysis was recently published [12].

4.2.1. Harmonic excitation In figure 8, we show again the amplitude and the phase shift of the induced currents for a excitation frequency of 480 Hz. The stronger deviation to the case of a homogeneous fluid are detected for the phase, while the amplitude is rather unaffected by the insertion of the torus.

4.2.2. Transient excitation In figure 9 we present again the measured and computed eddy current distribution for the case of pulsed excitation for the time instants 200, 600, 1000 and 1400 μs .

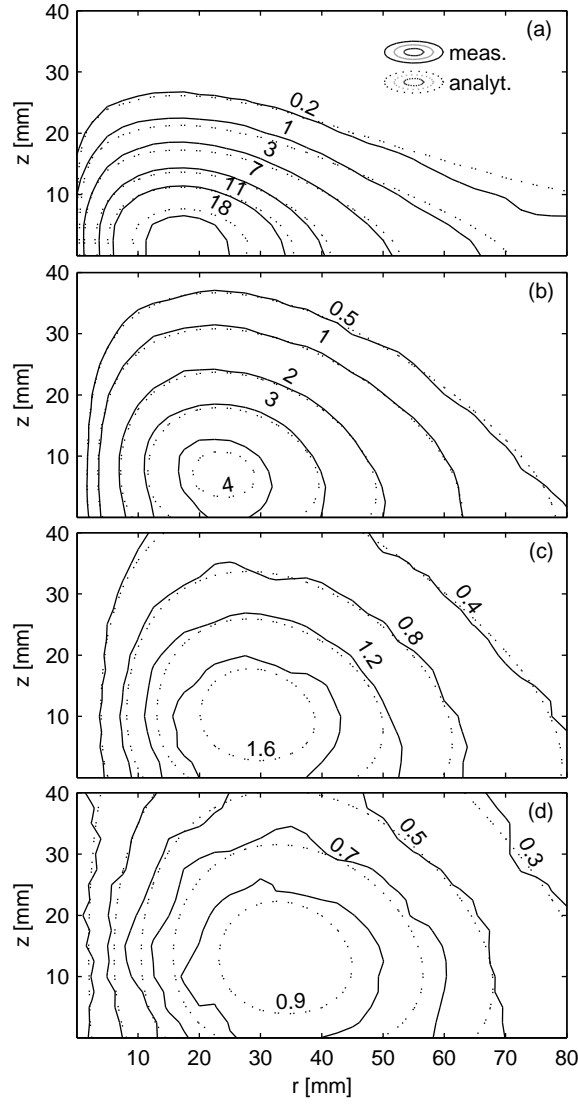


Figure 6. Contour-plot of the azimuthal eddy current-distribution [A/cm^2] in the case of pulsed excitation with an excitation current of 5 A. (a), (b), (c), (d) correspond to time instants, 200, 600, 1000, and 1400 μs , respectively. which were marked in figure 4.

The deviation of the measured total current from the numerically obtained one (figure 10) is a bit larger in this case, which might be due to the technical problems to measure the current close the inserted PVC ring.

5. Conclusions

We have measured the two-dimensional, axi-symmetric distribution of eddy currents in a liquid metal arising from harmonic or pulsed excitations in a nearby coil. In both

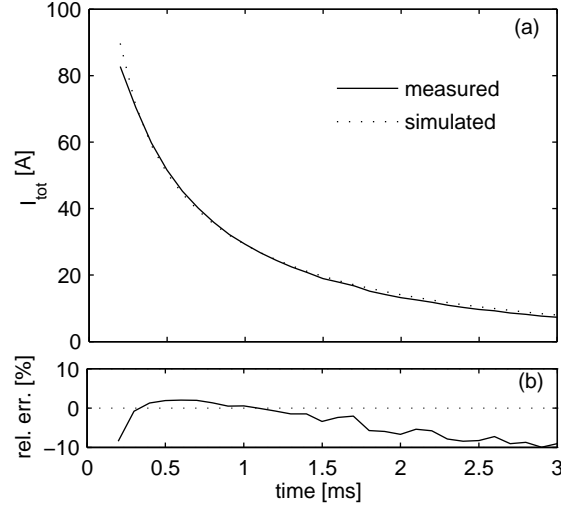


Figure 7. Time evolution of the total current for the pulsed current excitation in the case of a homogeneous fluid.

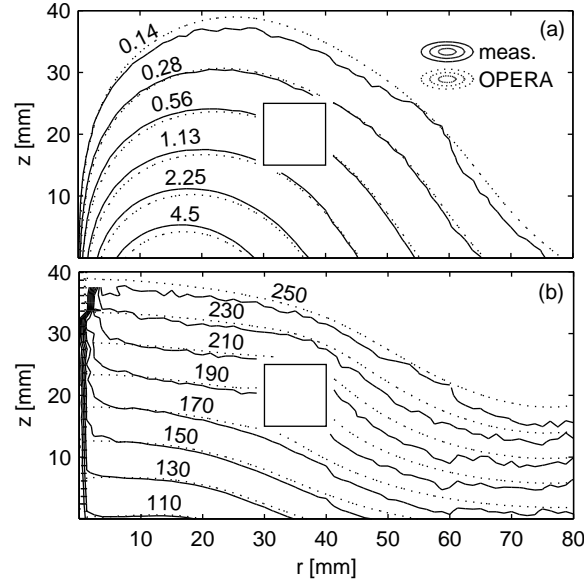


Figure 8. Inhomogeneous fluid: contour lines of amplitude [A/cm^2] (a) and phase-angle [$^\circ$] (b) of the azimuthal eddy current in the case of harmonic excitation with a frequency of 480 Hz and an excitation current of 1 A.

cases, the measured values show a satisfactory agreement with the analytical solution of the corresponding problem for a conducting half-space. Expectedly, a non-conducting torus immersed into the fluid disturbs the eddy current distribution, which was also confirmed by means of a commercial numerical solver (OPERA).

Although we have restricted our interest to axi-symmetric problems in which

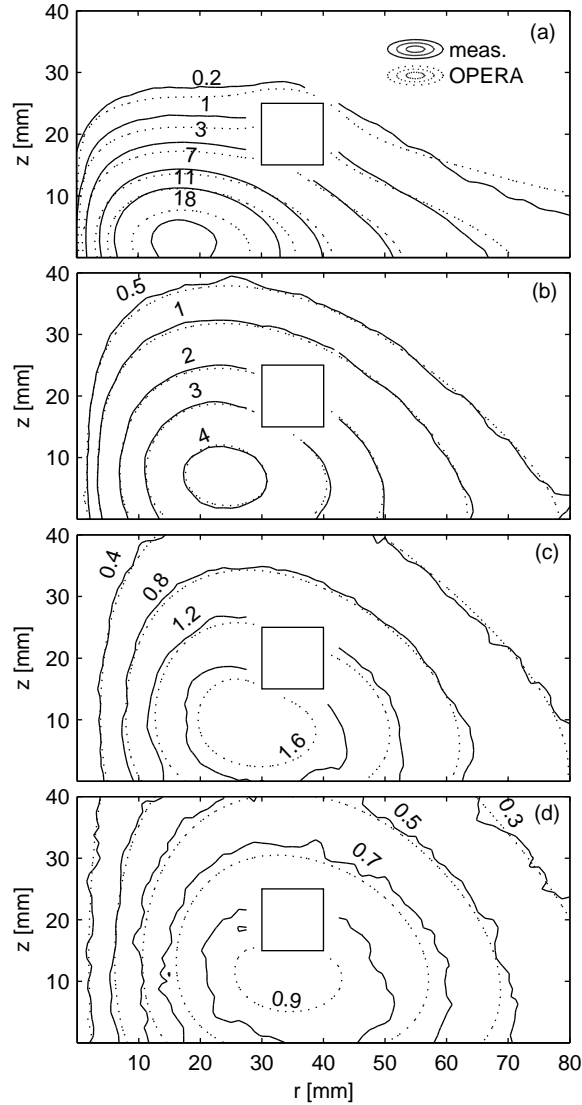


Figure 9. Case of an inserted PVC ring with quadratic cross-section: contour lines of the amplitude of the azimuthal eddy current in the case of pulsed excitation with a excitation current of 5 A. The full lines are the measured data, the dotted lines are the numerical ones. (a), (b), (c), (d) correspond to time instants, 200, 600, 1000, and 1400 μs , respectively.

the only relevant current component is the azimuthal one, the method can easily be generalized to fully three-dimensional scans of all three eddy current components. This way, it might help to validate numerical models for non-destructive testing and magnetic inductance tomography.

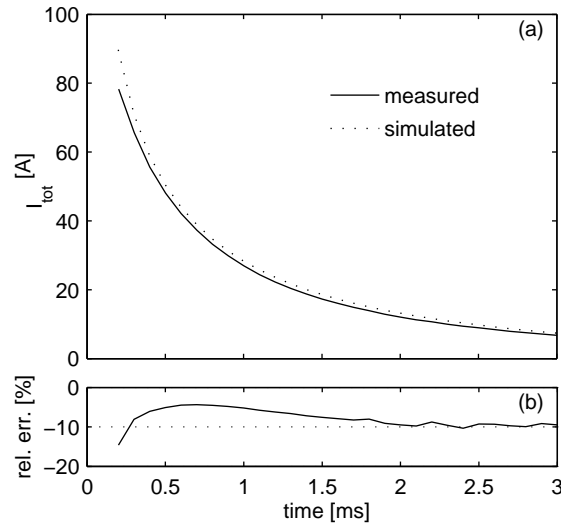


Figure 10. Time evolution of the total current for the pulsed current excitation in the case with an immersed PVC ring.

Acknowledgments

This work was supported by Deutsche Forschungsgemeinschaft in frame of the Sonderforschungsbereich 609.

References

- [1] Griffith H 2001 Magnetic induction tomography *Meas. Sci. Technol.* **12** 1126-31
- [2] Blitz J 1997 *Electrical and Magnetic Methods of Non-destructive Testing* Springer: Berlin
- [3] Stefani F and Gerbeth G 2000 A contactless method for velocity reconstruction in electrically conducting fluids *Meas. Sci. Technol.* **11** 758-65
- [4] Stefani F, Gundrum T and Gerbeth G 2004 Contactless inductive flow tomography *Phys. Rev. E* **70** 056306
- [5] Priede J, Buchenau D and Gerbeth G 2006 Contactless electromagnetic induction flowmeter based on phase shift measurements *Proc. 5th Int. Symp. Electromagnetic Processing of Materials (EPM2006)* (ISIJ, Tokyo) p 735
- [6] Thess A, Votyakov E V and Kolesnikov Y 2006 Lorentz force velocimetry *Phys. Rev. Lett.* **96** 164501
- [7] Fujiwara K and Nakata T 1990 *COMPEL* **9** 137
- [8] Förster F 1996 *Nondestructive Testing Handbook* Vol. 4, 2nd edn, American Society for Nondestructive Testing: Columbus OH, sections 4 and 5
- [9] Blitz J and Alagoa K D 1985 Eddy-current testing of Wood's metal models for inclined cracks *NDT Intern.* **18** 269-73
- [10] Smith RA and Hugo G R 2001 *Insight* **41** 14-25
- [11] Tegopoulos J A and Kriezis E E 1985 *Eddy Currents in Linear Conducting Media* Elsevier: Amsterdam
- [12] Tsuboi H, Seshima N, Sebestyen I, Pavo J, Gyimothy S, and Gasparics A 2004 *IEEE Trans. Magn.* **40** 1330-1333